Condensed tannin-glucose-based NIPU bio-foams of improved fire retardancy

Xinyi Chen, Jinxing Li, Xuedong Xi, Antonio Pizzi, Xiaojian Zhou, Emmanuel Fredon, Guanben Du, Christine Gerardin

Condensed Tannin-glucose-based NIPU Bio-Foams of Improved Fire Retardancy

Xinyi Chen[1]†, Jinxing Li[2]†, Xuedong Xi[1], Antonio Pizzi[1]*, Xiaojian Zhou[2], Emmanuel Fredon[1], Guanben Du[2], Christine Gerardin[3]

1 LERMAB, University of Lorraine, 27 rue Philippe Seguin, BP 1041, 88051 Epinal, France

2 Yunnan Provincial Key Laboratory of Wood Adhesives and Glued Products, Southwest Forestry University, Kunming, Yunnan province, China

3 LERMAB, University of Lorraine, Boulevard does aiguillettes, 54000 Nancy, France

* *Corresponding Author: Antonio PIZZI. Tel.: +33-623126940. E-mail address: antonio.pizzi@univ-lorraine.fr*

† *These authors contributed equally to this work.*

Abstract:

Glucose-based self-blowing non-isocyanate polyurethanes foams were prepared in our previous work. They showed excellent properties comparable to commercial foams by just using a simple preparation procedure. These foams, nevertheless, present a critical drawback that is their flammability. In the research presented here a natural phenolic compound, condensed tannin, was tested as a flame-retardant to improve the fire resistance of glucose-based NIPU foams. A number of tannin-substituted glucose-based NIPU foams (mimosa tannin replacing glucose at 0%, 25% and 50%, respectively) were prepared and characterized by scanning electron microscopy (SEM), Fourier transform infrared spectroscopy (FT-IR), Thermogravimetric analysis (TG), ignition experiment and limiting oxygen index (LOI). Other physical and mechanical properties, such as foaming processes, density, compression strength, etc. were also investigated. The results indicated that the tannin-modified glucose-based NIPU foams (T/G (1/3)-Fs and (T/G (1/1)-Fs)) exhibit smaller mean cell size, improved compression strength and higher density than (T/G (0/4)-Fs). The FT-IR analysis showed that urethane linkages were formed, the chemical structure of glucose-based NIPU foam being nonetheless preserved even if the glucose was partially replaced by the condensed tannin. Thermogravimetric analysis showed that the presence of condensed tannin decreased the thermal stability of the tannin-glucose NIPU foam composites slightly. In addition, ignition experiments were also carried out in which the glucose-based NIPU foams with a condensed tannin showed longer burning time than neat (T/G (0/4)-Fs). Finally,

limiting oxygen index (LOI) values from 17.5% to 25.5%, show a higher value with the increasing condensed tannin substitution.

Key words:

condensed tannin, biomass foam, fire resistance, glucose-based NIPU, compressive strength

1 Introduction

Polyurethane foams (PUs), being light-weight, and presenting excellent insulating property, as well as superior mechanical properties, have been extensively utilized in buildings as thermal and acoustic insulation materials [1-3]. However, PUs exhibit substantial drawbacks, including toxic and expensive raw materials, flammability and dripping after combustion, even though they are widely utilized [4].

Demands for safer, non-toxic and inexpensive materials have driven researchers to explore new technologies and starting materials. Lignin [5-7], tannin [8-10], sugar [11, 12], forestry and agriculture waste [6, 13, 14] and other natural hydroxy-carrying compounds, are typical biomass resources that as partial or complete replacement of petroleum-based polyhydric alcohols have been tried to prepare PUs. It is the most commonly utilized strategy and this kind of foams is known, incorrectly, as “bio-foams”. Besides, another one is that non-isocyanate strategies for PU foams have been reported in the literature [15, 16]. For example, such a latter approach used easily available, cost-effective materials and methods, such as the aminolysis of five-membered cyclic carbonates, to replace isocyanate when making PUs [4, 17-22]. Unfortunately, some shortcomings were still discovered, including harsh reaction conditions and environment (high temperature, catalyst) [23], high toxic reagent (epichlorohydrin) [22] and high pressure [18, 20].

We had initially sought a more environment friendly preparation strategy recently. Fortunately, a bio-mass resource-based (mimosa tannin, a condensed tannin), low

temperature (around 90 °C) and atmospheric pressure synthesis route was found [24, 25]. Meanwhile, the glucose-based NIPUs so prepared have been used for wood coatings and wood bonding as well as to prepare foams [11, 12, 26]. The open cell foams obtained by high-temperature induced foaming has excellent properties, and its cellular structure is recovered after the pressure on it is released, even if the cell walls were flattened by compression.

Nevertheless, in common with traditional PUs, the all glucose-based NIPU foams, regardless if obtained at high temperature or room temperature, are flammable [12, 26]. This limits their applications as fire resistance materials. Therefore, to improve their fire resistance still remained the key aim of the research work presented here. The literature reports that numerous types of flame retarding additive can improve the fire resistance of materials effectively, for instance, halogenated compounds [27], phosphorus-containing compounds [28, 29] and nano-additives [30-34]. They either trigger a flame retarding barrier, or play a role as a layer blocking flammable gases, or both [35]. However, they will release toxic halogen- or phosphorus-containing gases which can threaten the environment during burning and the foam properties will deteriorate because of the high content of additives.

Nowadays, some researchers have turned their attention to bio-based flame retardants, such as tannin [36, 37], caseins [38], phytic acid [39] and banana pseudo-stem sap liquid [40]. Tannins became the first candidate bio resourced material, which can be obtain from the bark, seeds and other parts of plentiful species of trees [41-43]. Moreover, they

have many special properties such as antibacterial and antioxidant [44, 45], precipitate proteins [46], reductants and stabilizers [47]. It was reported that tannins can act as a natural fire resistance to aid tree survival [48]. This is mainly attributed to their similar reactivity to phenol, phenoxy radicals could quench the oxygen free radicals when the polymer is decomposed during heating [35]. In addition, tannins have high char production efficiency when burning (55% char for condensed tannin and 28% char for tannic acid) [37, 49, 50], resulting in a protective layer, which is made of char and can block heat, oxygen, and flammable gases [51]. At the same time, due to their effect, the tannins can increase the foam mechanical properties while acting as a fire retardant [35]. Thus, the work presented here is focused on condensed tannin as a natural fire retardant to improve the flame resistance of glucose-based non-isocyanate polyurethane foams. The resins and foams prepared were obtained at ambient pressure, at different ratios of glucose and tannin. The morphology and performance of glucose/tannin foams were investigated by SEM, FT-IR and TG and other techniques. The fire resistance of all foams was determined by means of direct ignition and limiting the oxygen index (LOI) measurement.

2. Materials and methods

2.1 Materials

Mimosa tannin extract is a commercial product, namely mimosa tannin extracted from the bark of *Acacia mearnsii (De Wild)*, supplied by Silva Chimica (St. Michele Mondovi, Italy). Glutaraldehyde ($C_5H_8O_2$, 50% water solution) was obtained from

Acros Organics, France; Glucose (99.99%, anhydrous), Hexamethylenediamine (HDMA, 98%), Dimethyl carbonate (DMC, 99%, anhydrous), Hexamethylenetetramine (99%, ACS reagent), Citric acid (99.5%, ACS reagent), were supplied by Sigma-Aldrich (Saint Louis, France). All these chemical reagents did not need any further purification before use. Deionized water (DI) was produced in the laboratory.

2.2. Preparation process

2.2.1 Preparation of the glucose or glucose-tannin-based Non-Isocyanate Polyurethanes (NIPUs)

The neat glucose or glucose-tannin-based NIPUs were prepared according to a procedure already reported [52]. Three kinds of NIPUs mixtures for foaming preparing were prepared in this work. Glucose or glucose/tannin mixture and deionized water were placed into three-necked flask with condensing reflux, magnetic stirring and thermometer. And then, dimethyl carbonate (DMC) was added into the mixture and stirred thoroughly, mixed evenly, and heated to 65 ℃ and remained for 1 h. Subsequently, 70% solution (in water) of hexamethylenediamine was added into the mixture under mechanical stirring, while the mixture was heated to 90 ℃ and remained for 2 h. Finally, the glucose or glucose-tannin-based NIPUs were obtained and cooled down to room temperature, standby application. The proportions of materials used are shown in Table 1.

Table 1 The formulation of glucose or glucose-tannin-based NIPUs

Samples	Tannin (g)	Glucose (g)	DMC (g)	HDMA (g)	Water (g)
T/G (0/4)-NIPUs	0	40	27	77.6	33.34
T/G (1/3)-NIPUs	10	30	27	77.6	33.34
T/G (1/1)-NIPUs	20	20	27	77.6	33.34

2.2.2 Foam preparation

All foam samples were prepared according to our previous work already reported [12]. 10 g of G-NIPUs or T/G-NIPUs and 1 g hexamethylenetetramine were added into a 100 mL plastic beaker and then stirred at for 1 min. 8 g of the complex acid blowing agent (citric acid: glutaraldehyde = 3:1) was added and then the mixtures were stirred at room temperature for 10-15 s. The as-obtained flexible foams were placed at in ambient environment until the foam structure trend to stable. According to the species of T/G (0/4)-NIPUs, T/G (1/3)-NIPUs and T/G (1/1)-NIPUs as utilized in the experiments, the obtained flexible foams were recorded as T/G (0/4)-Fs, T/G (0/4)-Fs and T/G (0/4)-Fs, respectively. Subsequently, all flexible foam samples were put into the oven overnight at 70-80 ℃ and were taken out from the plastic beakers. The final cured foam samples were placed at ambient temperature (25℃and 12% relative humidity) for 2 days prior to characterization.

2.3. Measurements

126 2.3.1 Behavior of foaming process

127 The behavior of the foaming process was investigated in terms of previous reported
128 [53]. The rising time (the time from pouring the complex acid blowing agent into the
129 NIPUs until full expansion of the resulting foam) and tack free time (the time from
130 pouring the complex acid blowing agent into the NIPUs until the skin of the foam was
131 no longer sticky) were two critical parameters of foaming process. A thermometer was
132 fixed and deposited into inner of T/G-NIPUs to measure the foaming temperature
133 changes in the foaming process. The rising time, tack free time and foaming
134 temperature were accurate recorded and monitored, respectively. Each foaming process
135 replicate was tested five times and average value was taken.

136 2.3.2 Fourier transform infrared (FT-IR) spectroscopy

137 The functional groups of all foam samples were analyzed with a PerkinElmer Frontier
138 ATR-FT-MIR provided by an ATR Miracle diamond crystal. The sample powders were
139 laid on the diamond eye (1.8 mm) of the ATR equipment and the contact for the sample
140 was ensured by tightly screwing the clamp device. Each sample was scanned registering
141 the spectrum with 32 scans with a resolution of 4 cm^{-1} in the wave number range
142 between 600 and 4000 cm^{-1}.

143 2.3.3 Scanning electron microscopy (SEM) observation

144 To investigate the cell microstructure and morphology of glucose or tannin-glucose-
145 based NIPUs foams, the scanning electron microscopy (Gemini SEM 300, Germany)
146 was used with an acceleration voltage of 10 kV. The cell morphologies were statistically

147 analyzed depend on the SEM images by Nano Measurer 1.2 [54]. The cell size
148 distributions of all foams were calculated. The abovementioned parameters were
149 calculated by averaging several tens of individual cells for each sample.

150 2.3.4 Apparent density

151 The apparent densities were obtained as the ratio of weight to cubic specimen volume,
152 according to ASTM D1622-08. The size of the samples was 30 mm × 30 mm × 30 mm.
153 The average of five samples was determined.

154 2.3.5 TG analysis

155 The thermal stability of the foams was measured by using a TGA5500 analyzer (TA
156 instruments, USA). Sample powder amounting to 5-8 mg was transferred to a platinum
157 pan, with the temperature ranging from 25℃ to 790℃ at a heating rate of 10 ℃·min^{-1}
158 in a nitrogen atmosphere.

159 2.3.6 Compression strength

160 The compression strength of the foams in the direction parallel to that of the foam rise
161 were determined under ambient conditions by using a universal testing machine
162 (Instron 3300, Elancourt, France). The size of the samples was 25 mm × 25 mm × 25
163 mm, and the crosshead rate was fixed at 2.0 mm·min^{-1} for each sample. At least three
164 samples were tested to determine the average value.

165 2.3.7 Direct ignition test

166 The direct ignition test was carried out according to a method already described in the
167 literature [12]. Foam samples were made to specification size, 30 mm × 30 mm × 30

mm, and then were exposed facially to a stainless-steel frame preheated on a Bunsen burner (around 1000°C). Making sure the samples were located in the outer flame area of the Bunsen burner. The burning time was calculated starting by the samples were placed on the burner, till the flame of sample was considered as extinguished. Subsequently, the sample chars were weighted and noted as quality of residue. All tests were carried out in a closed environment to minimize the influence of other factors. Each foam type was tested three times.

2.3.8 Limiting oxygen index (LOI)

The limiting oxygen index (LOI) was measured according to a method reported in the literature [53] using an HC-2 oxygen index meter (Jiangning Analysis Instrument Company, China). All samples were prepared to specification size of 80 mm ×10 mm × 10 mm. The LOI values used were the averages for the five samples.

3 Results and discussion

3.1 Preparation of Tannin-glucose-based NIPUs foams (T/G (0/4)-Fs, T/G (1/3)-Fs and T/G (1/1)-Fs)

The tannin-glucose-based NIPUs foams (T/G (0/4)-Fs, T/G (1/3)-Fs and T/G (1/1)-Fs) were prepared with ease at ambient temperature. The main foreseeable adducts formed by multiple reactions eventually leading to structural networks in the foam are shown in Scheme 1. The foaming process can be divided into two main processes: the first one is the foaming process. The energy in this stage was produced from the rather violent reaction with citric acid and -NH_2 groups (obtaining the adducts 6, 7 and 8), which

provides the self-blowing energy at room temperature [12]. The second one is the network crosslinking. Hexamethylenetetramine and glutaraldehyde act as crosslinkers to ensure that the liquid foam formed does not collapse and be maintained (obtaining the adducts 1, 2, 3, 4 and 5). And then, these adducts can further crosslink to form large molecules, which can intertwine with each other. Ultimately, this effect causes the sharp increase of the viscosity of the mixture and then its gelling, resulting in a three-dimensional network (cf. Scheme 2). In fact, these two processes occur almost simultaneously. The reason for this analysis is to better understand the whole foaming process.

3.2 Apparent density

The prepared liquid flexible foams so prepared need to be hardened by heating, which was necessary to obtain and measure stable physical properties. Consequently, tannin-glucose-based foams (T/G (0/4)-Fs, T/G (1/3)-Fs and T/G (1/1)-Fs) with stable properties were prepared and shown in Figure 1. Some subtle differences between these three foam types can be seen, such as apparent color, foam cell status and cells size. The foam structures will be discussed in the following section, by comparing the scanning electron microscopy (SEM) observation. All foams, once the tannin was introduced, showed a black/red surface color. The reason of this is the reddening of mimosa tannin under acid conditions. Moreover, the apparent densities of the foams (cf. Table 2) increased as a function of the increase in the proportion of tannin. Thus, 50% tannin substitution yielded foams (T/G (1/1)-Fs) with the higher density, approximately

210 0.25 g·cm^{-3}, while the T/G (0/4)-Fs without tannin presented the lower density, around
211 0.15 g·cm^{-3}. This increase in foam density is ascribed to the more rapid gelling with
212 tannin and glutaraldehyde resulting in a higher cross-linking level much earlier in the
213 foaming process. Moreover, hexamethylenetetramine can provide further cross-linking
214 with tannin when the soft foams are heat-hardened. Thus, it appears that the extent of
215 cross-linking progressively increases with the addition of tannin.

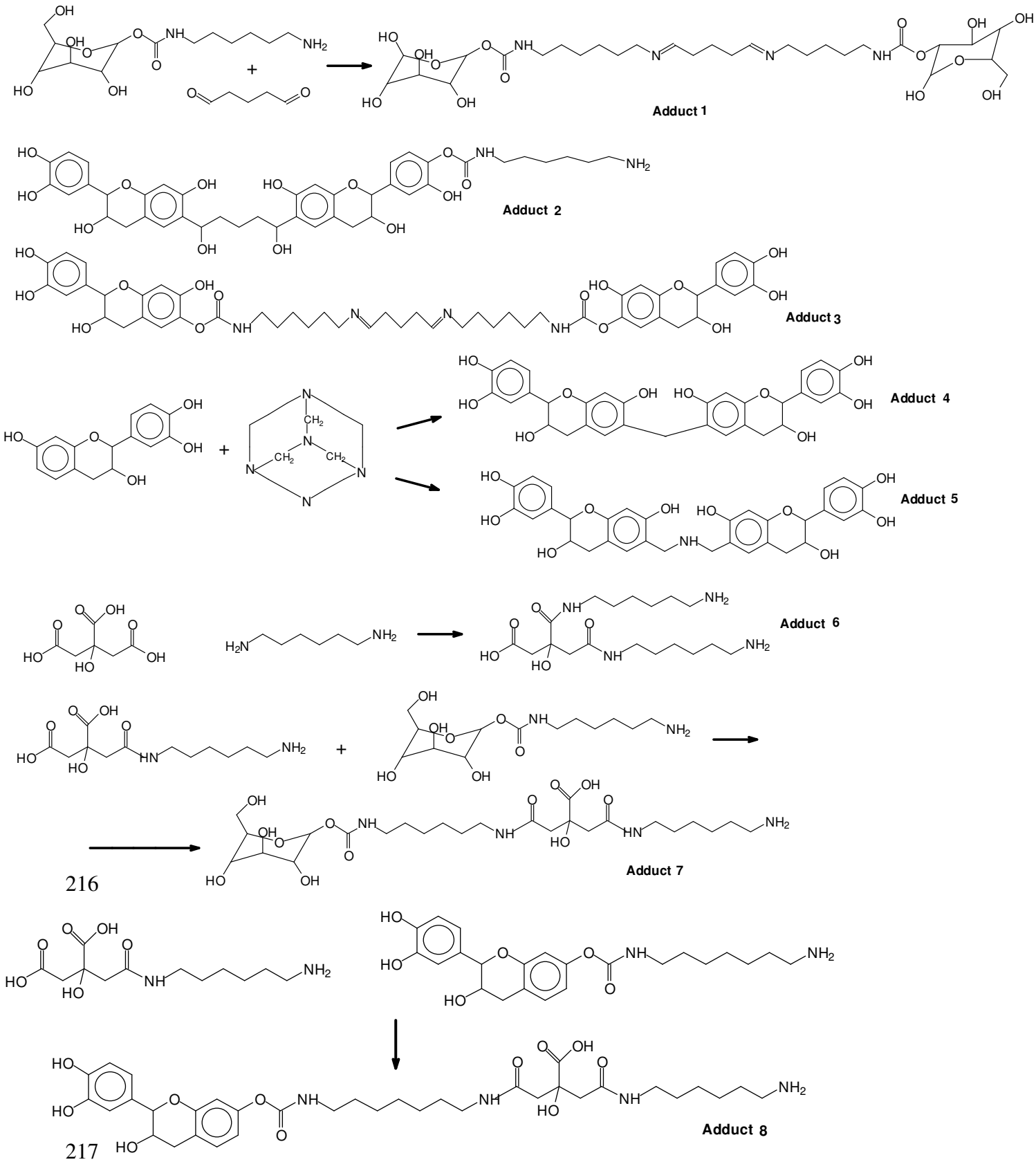

216

217

218 Scheme 1 The main foreseeable adducts formed by multiple reactions eventually

219 leading to structural networks in the foam.

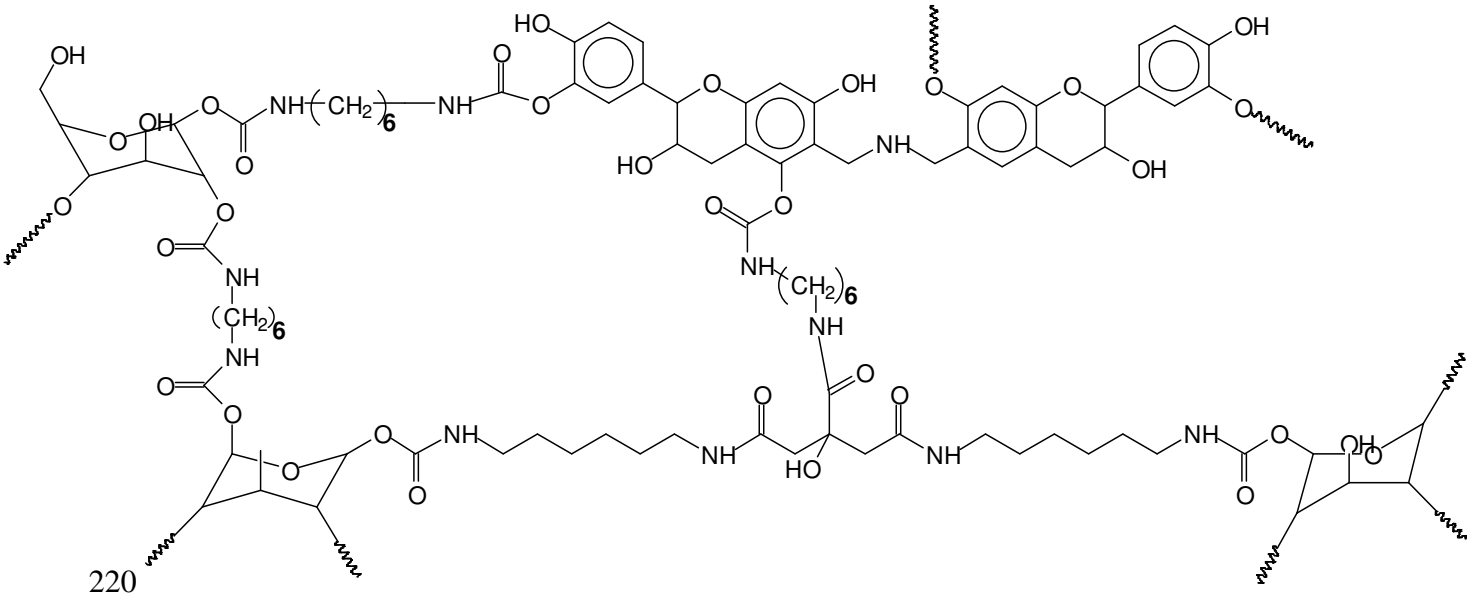

220

221 Scheme 2 A schematic example of some of the mixed linkages present in a possible

222 network structure of tannin/glucose foam

223

224 Figure 1 Digital images of three kinds of target foam samples. (a) T/G (0/4)-Fs; (b) T/G

225 (1/3)-Fs; (c) T/G (1/1)-Fs.

226 Table 2 Apparent density mean cell size and specific compressive strength of T/G (0/4)-

227 Fs, T/G (1/3)-Fs and T/G (1/1)-Fs

Samples	Apparent density (g cm^{-3})	Mean cell size (μm)	Specific compressive strength (kPa/kg m^{-3})

T/G (0/4)-Fs	0.15 ± 0.02	252.18 ± 41.55	1.22 ± 0.19
T/G (1/3)-Fs	0.19 ± 0.02	246.23 ± 49.19	1.27 ± 0.23
T/G (1/1)-Fs	0.25 ± 0.03	243.08 ± 50.40	1.51 ± 0.20

3.3 Fourier transform infrared (FT-IR) spectroscopy

Fourier Transform Infrared (FT-IR) spectra of all foams are shown in Figure 2, to investigate the functional groups changes occurring in these foam preparations. The results indicate that T/G (0/4)-Fs, T/G (1/3)-Fs and T/G (1/1)-Fs presents similar chemical structures, however, and quite distinct from neat tannin (red curve) and glucose (black curve). The main absorption peaks on the spectra were identified by arrows and imaginary segmented lines. In view of Figure 2, an intense broad absorption band between 3500 and 3100 cm^{-1} is characteristic of the -OH groups [16, 55]. This broad peak is clearly apparent in the FT-IR spectra of neat tannin and glucose as well. The 3337 cm^{-1} -N-H stretching peak is attributed to secondary amides, and concerns two kinds of reaction products obtained (one of them being urethane groups) [24]. Furthermore, there are two clear absorption peaks at 2930 cm^{-1} and 2856 cm^{-1}, especially in the NIPU foams, which are attributed to the C-H stretching vibration of -CH_2 and -CH_3 [16, 52]. As shown in Figure 2 (b), there is some strong evidence for the formation of carbamate bonds. Of these the 1702 cm^{-1} band was attributed to the

C=O from urethane groups and the 1645 cm^{-1} band to the C=O from ester groups [16, 52]. Moreover, the 1536 cm^{-1} band is also characteristic of the urethane group confirming the formation of carbamate structures [16]. In the FT-IR spectrum of neat tannin and glucose, nevertheless, these kinds of absorption peaks have not been detected. Such evidence shows that glucose-based NIPU foams are obtained by the non-isocyanate approach taken under atmospheric pressure and low temperature. Therefore, even if glucose was only partially replaced by condensed tannin, the chemical structure of glucose-based NIPUs foams does not appear to be affected.

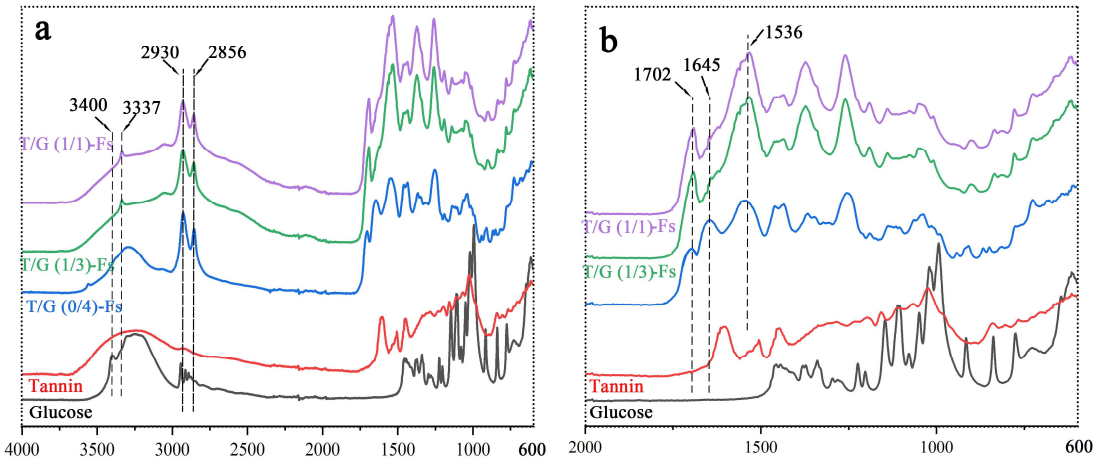

Figure 2 FT-IR spectra of neat tannin, glucose, glucose based NIPUs foam and tannin/glucose based NIPUs foam. (a) the wavenumber from 600-4000 cm^{-1}; (b) the wavenumber from 600-2000 cm^{-1}.

3.4 SEM analysis

SEM was used to investigate the foams morphology at different replacement levels of condensed tannin. The SEM images of the T/G (0/4)-Fs, T/G (1/3)-Fs and T/G (1/1)-Fs are shown in Figure 3. From this it appears that all foams present a regular cells morphology. A considerable number of open pores are observed in Figure 3 (a), (d) and

(g), attributed to water evaporation in the precursor resins during foaming and drying. Furthermore, some ruptures or debris also can be observed in all foams, these being ascribed to the cutting process in preparing the samples [54]. Comparing Figure 3(b) and Figure 3(e), (h), thicker cell walls were obtained with increasing the presence of condensed tannin. This phenomenon belongs to the thickening function of tannin-derived products on glucose-based NIPU foam. Furthermore, in Figure 3(f), (i), some fibrous polymers can also be clearly seen, interspersed in the cell wall or attached to their surfaces. These fibrous polymers as filler interspersed in glucose-based NIPU foam, resulted not only in an expansion effect that thickened the cell wall, but in the progressive increases of compression strength. As well as the number of fibrous polymers and cell walls thickness progressively increases by tannin addition the compression strength also progressively increases. Just because of this reason, the condensed modified foams obtained a smaller mean cell size (cf. Table 2).

According to literatures [55], condensed tannins have higher temperature (above 500°C) carbonization efficiency under an atmospheric environment. Therefore, in view of Figure 3(f), (i), the tannin-derived fibrous polymers inserted into, or covering the cell walls can be transformed into char or a char covering layer after high temperature decomposition. This is mainly attributed to their similar reactivity to phenol, phenoxy radicals being able to quench the oxygen free radicals when the polymer is decomposed during heating [35]. Therefore, the char so formed can either retard or even prevent effectively the combustion process of the foams. Conversely, without any tannin

addition a smooth fracture surface and inner surface of T/G (0/4)-Fs can be seen in Figure 3(c). Precisely due to this surface smoothness of T/G (0/4)-Fs, glucose-derived products alone do not have high carbonization efficiency so that they can only provide a limited protection during ignition and LOI testing. Hence, the interspersed and attached tannin-derived polymers in T/G (1/3)-Fs and T/G (1/1)-Fs cell wall can form a protecting char layer when these foams are exposed to high temperatures condition. These can well explain why in ignition experiments only a much smaller flame can be seen and a higher LOI was obtained for T/G (1/3)-Fs and T/G (1/1)-Fs foams, compared to T/G (0/4)-Fs.

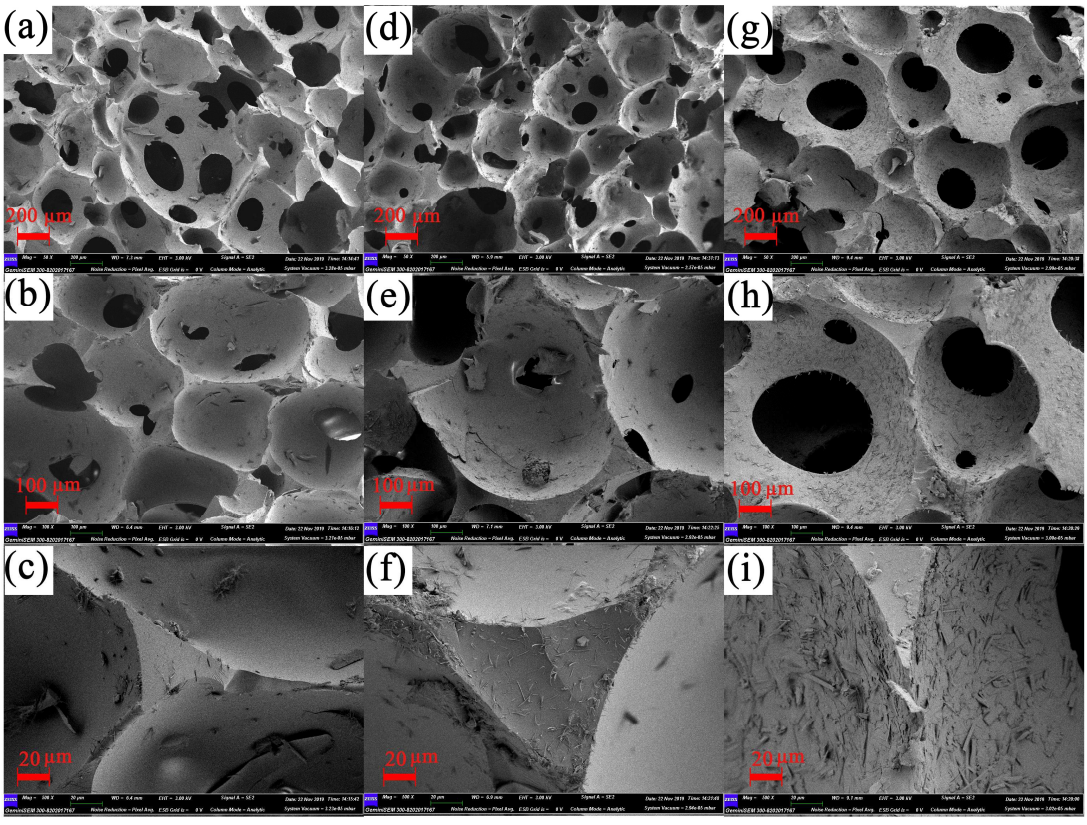

Figure 3 SEM images of the T/G (0/4)-Fs (a-c), T/G (1/3)-Fs (d-f) and T/G (1/1)-Fs (g-i)

293 3.5 Thermogravimetric analysis (TGA)

294 Thermogravimetric analysis (TGA) has been routinely used to evaluate the thermal
295 stability of various foams [54-57]. Thus, the TGA (a) and DTG (b) curves of T/G (0/4)-
296 Fs, T/G (1/3)-Fs and T/G (1/1)-Fs under N_2 atmosphere are shown in Figure 4. The
297 corresponding specific degradation temperatures and char yields at 790°C are listed in
298 Table 3. The T_{max} value reported in Table 3 is the maximum temperature shown by DTG
299 curves peaks at different pyrolysis stages. It can be observed that all foam samples
300 present a similar pyrolysis behavior, with two-stage decomposition which are typical of
301 the pyrolysis of polyurethane foams [58]. The first mass loss stage occurs within the
302 temperature range of 150°C-300°C, which belongs to the decomposition reaction of the
303 bond cleavage of urethane [56]. The second mass loss stage occurs between 380°C and
304 600°C, this been attributed to the breaking of C-C bonds and the further decomposition
305 of pyrolysis residual products from the first stage [55, 56]. It is still worth noting that
306 the DTG curve views a small peak at low temperature between 50°C and 100°C, which
307 may be ascribed to decompose of excess acid and hexamethylenetetramine, as well as
308 volatilize of absorbed water.

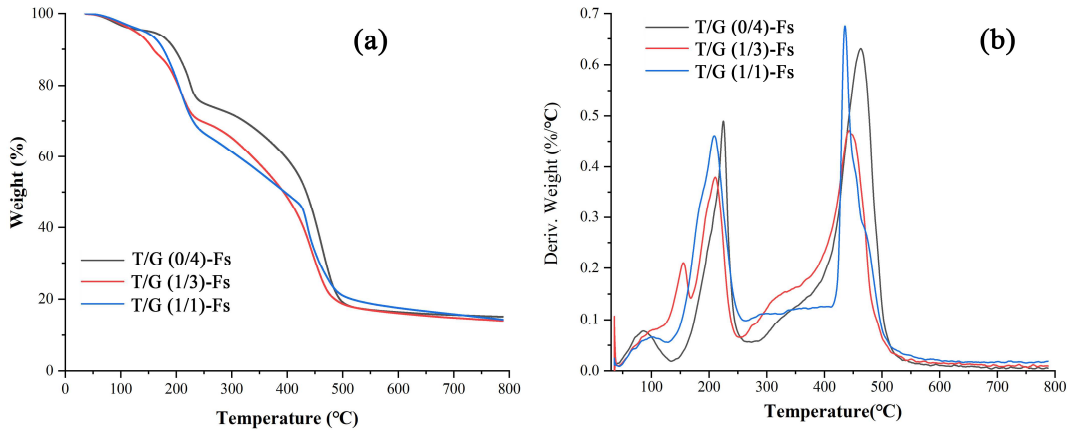

309

Figure 4 TGA (a) and DTG (b) curves of T/G (0/4)-Fs, T/G (1/3)-Fs and T/G (1/1)-Fs (under N_2 atmosphere)

In Figure 4, some significant differences can be observed when increasing the condensed tannin content, resulting in a slight decrease of the pyrolysis temperature of the foams. Nevertheless, the percentage value of the final residual mass at 790℃ indicates that all foam samples have a similar percentage mass loss, their residual mass being around 14-15% under a N_2 atmosphere. Between T/G (0/4)-Fs, T/G (1/3)-Fs and T/G (1/1)-Fs, a noticeable change can be seen, which is a shift of the decomposition temperature to lower temperatures, from 225°C (first stage) 462°C (second stage) decrease to 210°C (first stage) and 441°C (second stage) and 208 °C (first stage) 435°C (second stage), respectively (cf. Table 3). This is likely to be the initial thermal depolymerization of mimosa tannin extract at lower temperature, this occurring around 146℃ and the partial breakage of the intermolecular bonds of condensed tannin at around 450℃ [55]. This phenomenon was similar with others described in the literature [54, 55]. Therefore, condensed tannin addition reduced thermal stability of NIPU foams under a N_2 atmosphere.

Table 3 DTG data of T/G (0/4)-Fs, T/G (1/3)-Fs and T/G (1/1)-Fs (under N_2 atmosphere)

Samples	T_{max} (℃)		Residual mass at 790℃ (%)
	Step I	Step II	
T/G (0/4)-Fs	225	462	15.1
T/G (1/3)-Fs	210	441	14.4

T/G (1/1)-Fs	208	435	14.2

3.6 Compressive mechanical properties

Compression experiments were conducted to determine the effect of different tannin substitution on the compressive mechanical properties of glucose-based NIPU foams. The compressive stress-strain curves of T/G (0/4)-Fs, T/G (1/3)-Fs and T/G (1/1)-Fs samples are shown in Figure 5. The three-section curve is composed of three stages, namely the elastic behavior of the foam's cell wall bending(I), cell collapse(II) and densification(III) [59]. As shown in Figure 5, T/G (1/1)-Fs shows the highest compression strength and then T/G (1/3)-Fs and T/G (0/4)-Fs samples. The reason one for this is that the T/G (1/1)-Fs sample shows greater density then T/G (1/3)-Fs and T/G (0/4)-Fs samples, as the foams density is directly proportional to compression strength. This result echo those of many other studies, i.e. higher density leads in general to higher strength [8, 53]. In addition, the second reason is attributed to thicker cell walls of tannin modified foams (T/G (1/3)-Fs and T/G (1/1)-Fs), resulting to obtain a better compression loading distribution over the cell walls and thus an improved compression resistance [54]. Thicker cell walls originate from the tannin-derived products, which are interspersed within the foam cell walls and which tend to thicken the cell walls by their expanding action. This conclusion is supported by the results in Figure 3. Interestingly, there may still be another possible explanation for the higher compression properties. The inserted tannin-derived products may have served as a framework to improve the compression resistance as well.

According to the relevant literatures [54] and the tests described here, lower density foam samples have thinner cell walls, thereby they can only provide a rather limited contribution to compression resistance [60]. Thus, to investigate whether any upgrading in mechanical properties is only attributed to the increasing density of materials, the specific compressive strength of all foams was measured depending on the literature [53]. The specific compressive strength of all foam samples is shown in Table 2, which indicated that the specific strength exhibits the increasing trend with the increasing of condensed tannin addition. For T/G (0/4)-Fs, T/G (1/3)-Fs and T/G (1/1)-Fs samples, the corresponding of specific compressive strength is 1.22 kPa/kg m^{-3}, 1.27 kPa/kg m^{-3} and 1.51 kPa/kg m^{-3}, respectively. The results showed the improvement of mechanical properties of tannin modified-foams that this progress of strength is not exclusively attributed to the density alone, but related to the contribution of the cell wall [53]. This conclusion also justifies the above-mentioned analysis. Therefore, taking into account Table 3 and Figure 5, the results further indicate that the compression strength of these foams is improved by adding increasing proportions of condensed tannin.

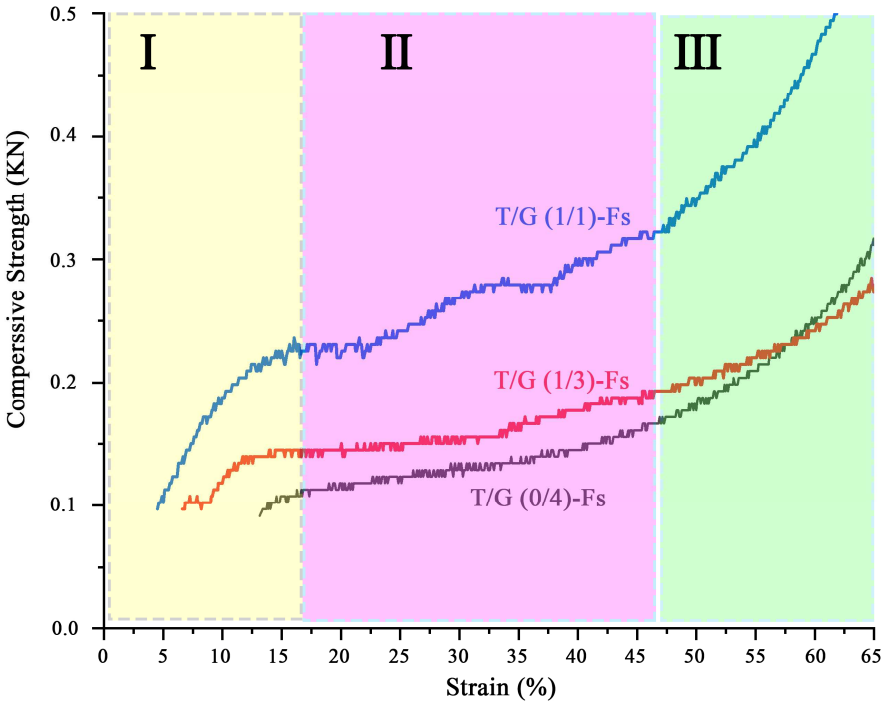

362

363 Figure 5 Compressive stress-strain curves of T/G (0/4)-Fs, T/G (1/3)-Fs and T/G

364 (1/1)-Fs

365 3.7 Ignition experiment of T/G (0/4)-Fs, T/G (1/3)-Fs and T/G (1/1)-Fs samples

366 Although there are some limitations in the fire resistance evaluation of the ignition

367 experiments reported here, they can indicate to a certain extent the combustion

368 resistance of the material. Therefore, we designed this test to investigate the

369 flammability of T/G (0/4)-Fs, T/G (1/3)-Fs and T/G (1/1)-Fs ignition combustion

370 experiments were conducted on the foam samples directly. The digital photos of

371 ignition experiments and the results are shown in Figure 6 and Table 4, respectively.

372 The burning time increased with the increase of tannin addition, from 175s for T/G

373 (0/4)-Fs to 245s for T/G (1/3)-Fs, and then 372s for T/G (1/1)-Fs. The burning time of

374 T/G (1/1)-Fs was more than twice longer of T/G (0/4)-Fs. This conclusion being also

375 related to the density of the foams [12]. Furthermore, the residual weight of the foam

samples after burning was also evaluated. The same trend as the burning time was observed, with the T/G (1/1)-Fs foam sample presenting the higher residual weight at 15.52 %. This is attributed to the higher char rate of condensed tannin when heating. Therefore, condensed tannin modified foams obtained longer burning time and higher residual mass.

Table 4 The results of the ignition experiments

Samples	Burning time (s)	Residue (g)	Residual (%)
T/G (0/4)-Fs	175 ± 11	0.13 ± 0.02	9.87 ± 0.13
T/G (1/3)-Fs	245 ± 10	0.15 ± 0.02	12.54 ± 0.09
T/G (1/1)-Fs	372 ± 18	0.34 ± 0.03	15.52 ± 0.15

As shown in Figure 6, T/G (0/4)-Fs and T/G (1/3)-Fs shows a high flammability and a very intense flame was observed in just a very short time (30s), when the foams are either devoid of tannin or have a lower tannin content. Simultaneous, in this case a large number of black fumes (dotted blue frame) was released while the foam was burning. T/G (0/4)-Fs (Figure 6 (b)) and T/G (1/3)-Fs (Figure 6 (a)) samples do not show major differences in combustion flame. This is similar to traditional isocyanate-based polyurethane foams, indicating that these two foams are a highly flammable. However, the final burning product of T/G (1/3)-Fs samples can be maintained approximately in its original shape, compared to the completely irregular residue shape of T/G (0/4)-Fs. In addition, the combustion behavior of T/G (1/1)-Fs, shows a delicate small flame of which can be seen at the beginning of the burning experiment, are shown in Figure 6(c).

The intense flame and black fumes of T/G (0/4)-Fs and T/G (1/3)-Fs cannot be seen, from the beginning to the end of the experiment. Furthermore, the final product after burning keeps the original shape as well. These combustion phenomena show that while T/G (0/4)-Fs or T/G (1/3)-Fs and T/G (1/1)-Fs are all combustible, nevertheless, the ignitability is markedly lower when condensed tannin addition reached a certain proportion. All this suggests that condensed tannin have a certain inhibitory effect on the combustion behavior of T/G-Fs foam.

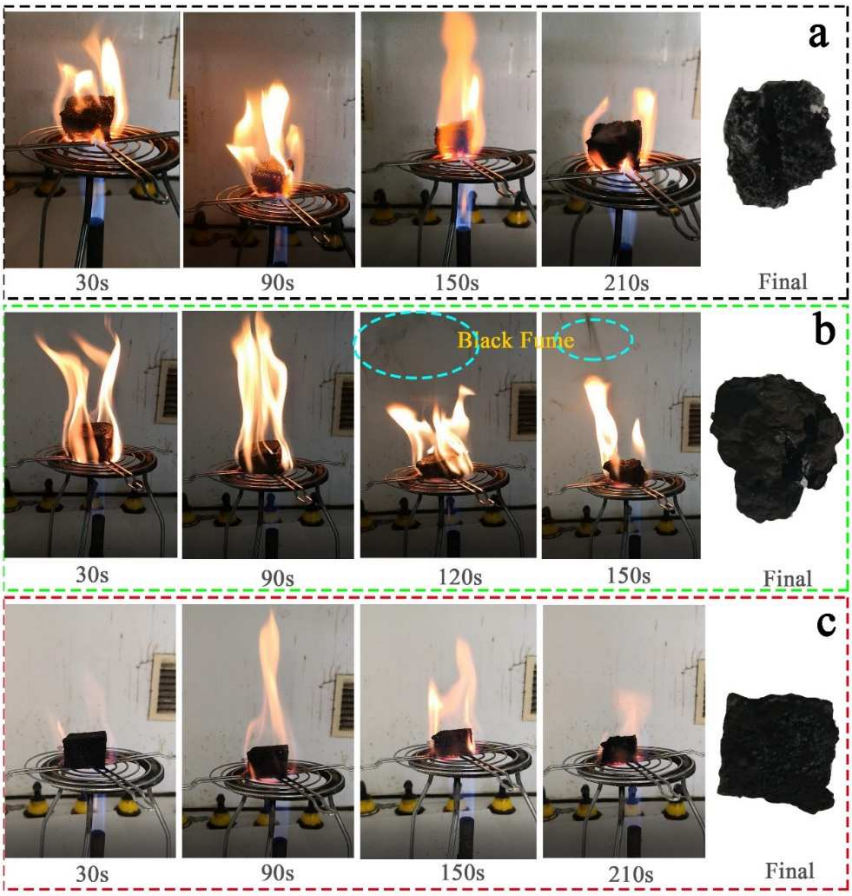

Figure 6 The digital photos of ignition experiments: (a) T/G (1/3)-Fs; (b) T/G (0/4)-Fs; (c) T/G (1/1)-Fs

3.8 Limiting oxygen index (LOI)

The limiting oxygen index (LOI) reflects the minimum oxygen concentration while the

polymer is burning in the mixed oxygen and nitrogen atmosphere to evaluate effectively the flame retardancy in polymers [54]. A material can be defined as flame-retardant when its LOI value is greater than 27%. Conversely, it can be defined as inflammable when its LOI value is less than 22% [61]. The LOI values of each foam samples were then evaluated and the results obtained are shown in Figure 7. The LOI values of neat glucose-based NIPU foam (T/G (0/4)-Fs*)* are around 17.5 %, indicating that this kind of foam belong to the class of inflammable materials, needing additional flame retardants to improve its fire resistance if we want to expend its application field [12]. As expected, the condensed tannin-glucose NIPU foams, T/G (1/3)-Fs and T/G (1/1)-Fs, presented improved LOI values of 20.0 % and 25.5 %, respectively. The cause of this improved results is probably attributed to the presence of the condensed tannin, which have a considerable proportion of aromatic rings. Therefore, the condensed tannin-glucose NIPU foams are more easily carbonized when the carbon atoms reach a high proportion level [35, 54, 62, 63]. In addition, from the structure of all foams, due to the enlarged cells (lower density) and a greater number of perforations of G-Fs (as shown in Figure 3(a), (d) and (g)), the oxygen can enter to the inner parts of the foam, thereby increasing the oxygen concentration and thus rendering the foam more inflammable [54]. Combined with the SEM images, the tannin-derived fibrous polymers either interspersed in the cell walls of T/G (1/3)-Fs and T/G (1/1)-Fs or covering them may well be the one of critical factors of the improved fire resistance of these foams. Exactly as explained above, these tannin-derived fibrous polymers can

then be easily converted into a char layer to improve the fire resistance of tannin-glucose-based NIPU foams. The ignition experiment results of all foam samples does also support such a conclusion. Therefore, the addition of condensed tannin can improve the LOI values of T/G (0/4)-Fs.

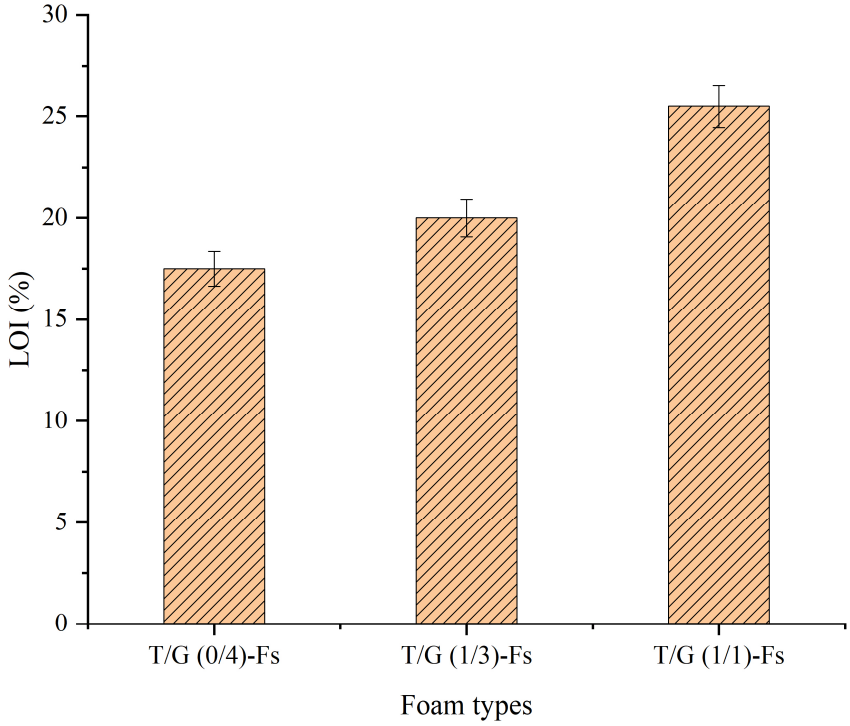

Figure 7 LOI of T/G (0/4)-Fs, T/G (1/3)-Fs and T/G (1/1)-Fs

4 Conclusions

Condensed tannin as a natural flame retardant to modify the fire resistance of glucose-based NIPU foam was investigated. It is concluded that the presence of mimosa tannin substituting different proportions of glucose in the NIPU foam can improve the ignitability of glucose-based NIPU foams. FT-IR results indicated that urethane linkages were formed in all foam formulations. The three kind of foams exhibited similar regular cell morphology, i.e. plenty of open pores can be seen clearly, but the T/G (1/3)-Fs and T/G (1/1)-Fs foams had smaller mean cell sizes than the T/G (0/4)-Fs.

The compressive mechanical properties were all enhanced on account of the different amount replacement of glucose by condensed tannin. The thermal stability of T/G (1/3)-Fs and T/G (1/1)-Fs with added condensed tannin decreased then T/G (0/4)-Fs. However, the ignition experiment shows that with an increasing proportion of condensed tannin, the burning time lengthened, from 175s for T/G (0/4)-Fs to 372s for T/G (1/1)-Fs, respectively. The LOI values were determined to investigate the fire resistance of glucose-based NIPU foams, indicating that T/G (1/1)-Fs obtained the highest LOI value (25.5%, still belonging to the combustible grade, but not to the inflammable range) due to its highest condensed tannin content. Conversely, the LOI values of neat glucose-based NIPU foams (T/G (0/4)-Fs) are around 17.5 %, belonging to inflammable grade. It can be seen from this, that condensed tannin can improve the fire resistance of T/G (0/4)-Fs, and yield better mechanical properties. This low-cost and highly effective biobased self-blowing glucose-/tannin-based foam presents a definite potential for practical application.

5 Acknowledgement

This work was supported by the Yunnan Provincial Natural Science Foundation (2017FB060), National Natural Science Foundation of China (NSFC 31760187), Scholarship from China Scholarship Council (CSC), Yunnan Provincial Key Laboratory of Wood Adhesives and Glued Products and The LERMAB is supported by a grant of the French Agence Nationale de la Recherche (ANR) as part of the laboratory of excellence (LABEX) ARBRE.

6 Reference

[1] Qian L, Li L, Chen Y, Xu B, Qiu Y. Quickly self-extinguishing flame retardant behavior of rigid polyurethane foams linked with phosphaphenanthrene groups. Composites Part B: Engineering 2019;175:107186. https://doi.org/10.1016/j.compositesb.2019.107186.

[2] Nuño P, Bulnes FG, Granda JC, Suárez FJ, García DF. A Scalable WebRTC Platform based on Open Technologies. 2018 International Conference on Computer, Information and Telecommunication Systems (CITS) 2018:1-5. https://doi.org/10.1109/CITS.2018.8440161

[3] Gama N, Costa LC, Amaral V, Ferreira A, Barros-Timmons A. Insights into the physical properties of biobased polyurethane/expanded graphite composite foams. Composites Science and Technology 2017;138:24-31. https://doi.org/10.1016/j.compscitech.2016.11.007.

[4] Bourguignon M, Thomassin J-M, Grignard B, Jerome C, Detrembleur C. Fast and Facile One-Pot One-Step Preparation of Nonisocyanate Polyurethane Hydrogels in Water at Room Temperature. ACS Sustainable Chemistry & Engineering 2019;14(7):12601-12610. https://doi.org/10.1021/acssuschemeng.9b02624.

[5] Wang Y-Y, Wyman CE, Cai CM, Ragauskas AJ. Lignin-Based Polyurethanes from Unmodified Kraft Lignin Fractionated by Sequential Precipitation. ACS Applied Polymer Materials 2019;1(7):1672-1679. https://doi.org/10.1021/acsapm.9b00228.

[6] Wadekar M, Eevers W, Vendamme R. Influencing the properties of Lignin PU films

by changing copolyol chain length, lignin content and NCO/OH mol ratio. Industrial Crops and Products 2019;141:111165. https://doi.org/10.1016/j.indcrop.2019.111655.

[7] Gómez-Fernández S, Günther M, Schartel B, Corcuera MA, Eceiza A. Impact of the combined use of layered double hydroxides, lignin and phosphorous polyol on the fire behavior of flexible polyurethane foams. Industrial Crops and Products 2018;125:346-359. https://doi.org/10.1016/j.indcrop.2018.09.018.

[8] Tondi G, Zhao W, Pizzi A, Du G, Fierro V, Celzard A. Tannin-based rigid foams: a survey of chemical and physical properties. Bioresource technology 2009;100(21):5162-5169. https://doi.org/10.1016/j.biortech.2009.05.055.

[9] Basso MC, Giovando S, Pizzi A, Pasch H, Pretorius N, Delmotte L, Celzard A. Flexible-elastic copolymerized polyurethane-tannin foams. Journal of Applied Polymer Science 2014;131(13): 40499. https://doi.org/10.1002/app.40499.

[10] Khundamri N, Aouf C, Fulcrand H, Dubreucq E, Tanrattanakul V. Bio-based flexible epoxy foam synthesized from epoxidized soybean oil and epoxidized mangosteen tannin. Industrial Crops and Products 2019;128:556-565. https://doi.org/10.1016/j.indcrop.2018.11.062.

[11] Xi X, Wu Z, Pizzi A, Gerardin C, Lei H, Zhang B, Du G. Non-isocyanate polyurethane adhesive from sucrose used for particleboard. Wood Science and Technology 2019;53(2):393-405. https://doi.org/10.1007/s00226-019-01083-2.

[12] Xi X, Pizzi A, Gerardin C, Lei H, Chen X, Amirou S. Preparation and Evaluation of Glucose Based Non-Isocyanate Polyurethane Self-Blowing Rigid Foams. Polymers

503 2019;11(11):1802. https://doi.org/10.3390/polym11111802.

504 [13] Wang H, Chen H-Z. A novel method of utilizing the biomass resource: Rapid
505 liquefaction of wheat straw and preparation of biodegradable polyurethane foam (PUF).
506 Journal of the Chinese Institute of Chemical Engineers 2007;38(2):95-102.
507 https://doi.org/10.1016/j.jcice.2006.10.004.

508 [14] dos Santos RG, Carvalho R, Silva ER, Bordado JC, Cardoso AC, do Rosário Costa
509 M, Mateus, MM. Natural polymeric water-based adhesive from cork liquefaction.
510 Industrial Crops and Products 2016;84:314-319.
511 https://doi.org/10.1016/j.indcrop.2016.02.020.

512 [15] Vanbiervliet E, Fouquay S, Michaud G, Simon F, Carpentier J-F, Guillaume SM.
513 Non-Isocyanate Polythiourethanes (NIPTUs) from Cyclodithiocarbonate Telechelic
514 Polyethers. Macromolecules 2019;52(15):5838-5849.
515 https://doi.org/10.1021/acs.macromol.9b00695.

516 [16] He X, Xu X, Wan Q, Bo G, Yan Y. Solvent- and Catalyst-free Synthesis,
517 Hybridization and Characterization of Biobased Nonisocyanate Polyurethane (NIPU).
518 Polymers 2019;11(6):1026. https://doi.org/10.3390/polym11061026.

519 [17] Dannecker PK, Meier MAR. Facile and Sustainable Synthesis of Erythritol
520 bis(carbonate), a Valuable Monomer for Non-Isocyanate Polyurethanes (NIPUs).
521 Scientific reports 2019;9(1):1-6. https://doi.org/10.1038/s41598-019-46314-5.

522 [18] Lee A, Deng Y. Green polyurethane from lignin and soybean oil through non-
523 isocyanate reactions. European Polymer Journal 2015;63,67-73.

524 https://doi.org/10.1016/j.eurpolymj.2014.11.023.
525 [19] Cornille A, Michaud G, Simon F, Fouquay S, Auvergne R, Boutevin B, Caillol S.
526 Promising mechanical and adhesive properties of isocyanate-free
527 poly(hydroxyurethane). European Polymer Journal 2016;84:404-420.
528 https://doi.org/10.1016/j.eurpolymj.2016.09.048.
529 [20] Esmaeili N, Vafayan M, Salimi A, Zohuriaan-Mehr MJ. Kinetics of curing and
530 thermo-degradation, antioxidizing activity, and cell viability of a tannic acid based
531 epoxy resin: From natural waste to value-added biomaterial. Thermochimica Acta 2017;
532 655:21-33. https://doi.org/10.1016/j.tca.2017.06.005.
533 [21] Tryznowski M, Świderska A, Gołofit T, Żołek-Tryznowska Z. Wood adhesive
534 application of poly(hydroxyurethane)s synthesized with a dimethyl succinate-based
535 amide backbone. RSC Advances 2017;7(48):30385-30391.
536 https://doi.org/10.1039/C7RA05455F.
537 [22] Esmaeili N, Zohuriaan-Mehr MJ, Salimi A, Vafayan M, Meyer W. Tannic acid
538 derived non-isocyanate polyurethane networks: Synthesis, curing kinetics,
539 antioxidizing activity and cell viability. Thermochimica Acta 2018;664:64-72.
540 https://doi.org/10.1016/j.tca.2018.04.013.
541 [23] Liu G, Wu G, Huo S, Jin C, Kong Z. Synthesis and properties of non-isocyanate
542 polyurethane coatings derived from cyclic carbonate-functionalized polysiloxanes.
543 Progress in Organic Coatings 2017;112:169-175.
544 https://doi.org/10.1016/j.porgcoat.2017.07.013.

545 [24] Thébault M, Pizzi A, Essawy HA, Barhoum A, Van Assche G. Isocyanate free
546 condensed tannin-based polyurethanes. European Polymer Journal 2015; 67:513-526.
547 https://doi.org/10.1016/j.eurpolymj.2014.10.022.
548 [25] Thébault M, Pizzi A, Santiago-Medina FJ, Al-Marzouki FM, Abdalla S.
549 Isocyanate-Free Polyurethanes by Coreaction of Condensed Tannins with Aminated
550 Tannins. Journal of Renewable Materials 2017;5(1):21-29.
551 https://doi.org/10.7569/JRM.2016.634116.
552 [26] Xi X, Pizzi A, Gerardin C, Du G. Glucose-Biobased Non-Isocyanate Polyurethane
553 Rigid Foams. Journal of Renewable Materials 2019; 7(3):301-312.
554 https://doi.org/10.32604/jrm.2019.04174.
555 [27] Lenoir D, Kampke-Thiel K. In: Gordon L. Fire and Polymers II, Vol. 599:
556 Formation of polybrominated dibenzodioxins and dibenzofurans in laboratory
557 combustion processes of brominated flame retardants. Washington, DC: American
558 Chemical Society, 1995. Chapter 25. pp 377-392. https://doi.org/10.1021/bk-1995-
559 0599.ch025.
560 [28] Schartel B, Balabanovich A, Braun U, Knoll U, Artner J, Ciesielski M, Döring M,
561 Perez R, Sandler JKW, Altstädt V, Hoffmann T, Pospiech D. Pyrolysis of epoxy resins
562 and fire behavior of epoxy resin composites flame-retarded with 9, 10-dihydro-9-oxa-
563 10-phosphaphenanthrene-10-oxide additives. Journal of applied polymer science 2007;
564 104(4):2260-2269. https://doi.org/10.1002/app.25660.
565 [29] Zhang W, Li X, Yang R. Pyrolysis and fire behaviour of epoxy resin composites

566 based on a phosphorus-containing polyhedral oligomeric silsesquioxane (DOPO-
567 POSS). Polymer degradation and stability 2011;96(10):1821-1832.
568 https://doi.org/10.1016/j.polymdegradstab.2011.07.014.
569 [30] Hussain M, Varley RJ, Mathys Z, Cheng YB, Simon GP. Effect of organo-
570 phosphorus and nano-clay materials on the thermal and fire performance of epoxy
571 resins. Journal of applied polymer science 2004; 91(2):1233-1253.
572 https://doi.org/10.1002/app.13267.
573 [31] Lee SK, Bai BC, Im JS, In SJ, Lee Y-S. Flame retardant epoxy complex produced
574 by addition of montmorillonite and carbon nanotube. Journal of Industrial and
575 Engineering Chemistry 2010;16(6):891-895. https://doi.org/10.1016/j.jiec.2010.09.014.
576 [32] Becker CM, Gabbardo AD, Wypych F, Amico SC. Mechanical and flame-retardant
577 properties of epoxy/Mg-Al LDH composites. Composites Part A: Applied Science and
578 Manufacturing 2011;42(2):196-202.
579 https://doi.org/10.1016/j.compositesa.2010.11.005
580 [33] Kim M-J, Jeon I-Y, Seo J-M, Dai L, Baek J-B. Graphene phosphonic acid as an
581 efficient flame retardant. ACS Nano 2014;8(3):2820-2825.
582 https://doi.org/10.1021/nn4066395.
583 [34] Gu J, Liang C, Zhao X, Gan B, Qiu H, Guo Y, Yang X, Zhang Q, Wang D-Y. Highly
584 thermally conductive flame-retardant epoxy nanocomposites with reduced ignitability
585 and excellent electrical conductivities. Composites Science and Technology
586 2017;139:83-89. https://doi.org/10.1016/j.compscitech.2016.12.015.

587 [35] Kim Y-O, Cho J, Yeo H, Lee BW, Moon BJ, Ha Y-M, Jo, YR, Jung, YC. Flame
588 Retardant Epoxy Derived from Tannic Acid as Biobased Hardener. ACS Sustainable
589 Chemistry & Engineering 2019;7(4):3858-3865.
590 https://doi.org/10.1021/acssuschemeng.8b04851.
591 [36] Silveira MRd, Peres RS, Moritz VF, Ferreira CA. Intumescent Coatings Based on
592 Tannins for Fire Protection. Materials Research 2019;22(2):0433.
593 http://dx.doi.org/10.1590/1980-5373-mr-2018-0433.
594 [37] Nam S, Condon BD, Xia Z, Nagarajan R, Hinchliffe DJ, Madison CA. Intumescent
595 flame-retardant cotton produced by tannic acid and sodium hydroxide. Journal of
596 Analytical and Applied Pyrolysis 2017;126:239-246.
597 https://doi.org/10.1016/j.jaap.2017.06.003.
598 [38] Carosio F, Di Blasio A, Cuttica F, Alongi J, Malucelli G. Flame Retardancy of
599 Polyester and Polyester-Cotton Blends Treated with Caseins. Industrial & Engineering
600 Chemistry Research 2014;53(10):3917-3923. https://doi.org/10.1021/ie404089t.
601 [39] Laufer G, Kirkland C, Morgan AB, Grunlan JC. Intumescent Multilayer
602 Nanocoating, Made with Renewable Polyelectrolytes, for Flame-Retardant Cotton.
603 Biomacromolecules 2012;13(9):2843-2848. https://doi.org/10.1021/bm300873b.
604 [40] Basak S, Samanta KK, Saxena S, Chattopadhyay S, Narkar R, Mahangade R,
605 Hadge, GB. Flame resistant cellulosic substrate using banana pseudostem sap. Polish
606 Journal of Chemical Technology 2015;17(1):123-133. https://doi.org/10.1515/pjct-
607 2015-0018.

608 [41] Belgacem MN, Gandini A. Monomers, polymers and composites from renewable
609 resources.Netherland: Elsevier, 2008. Chapter 8. pp 179-200.
610 [42] Belgacem MN, Gandini A. Monomers, polymers and composites from renewable
611 resources.Netherland: Elsevier, 2008. Chapter 10-11. pp 225-272.
612 [43] Arbenz A, Avérous L. Chemical modification of tannins to elaborate aromatic
613 biobased macromolecular architectures. Green Chemistry 2015;17(5):2626-2646.
614 https://doi.org/10.1039/C5GC00282F.
615 [44] Ma M, Dong S, Hussain M, Zhou W. Effects of addition of condensed tannin on
616 the structure and properties of silk fibroin film. Polymer International 2017; 66(1):151-
617 159. https://doi.org/10.1002/pi.5272.
618 [45] Ekambaram SP, Perumal SS, Balakrishnan A. Scope of Hydrolysable Tannins as
619 Possible Antimicrobial Agent. Phytotherapy Research 2016;30(7):1035-1045.
620 https://doi.org/10.1002/ptr.5616.
621 [46] Adamczyk B, Salminen J-P, Smolander A, Kitunen V. Precipitation of proteins by
622 tannins: effects of concentration, protein/tannin ratio and pH. International Journal of
623 Food Science & Technology 2012;47(4):875-878. https://doi.org/10.1111/j.1365-
624 2621.2011.02911.x.
625 [47] Majumdar R, Bag BG, Ghosh P. Mimusops elengi bark extract mediated green
626 synthesis of gold nanoparticles and study of its catalytic activity. Applied Nanoscience
627 2016;6(4):521-528. https://doi.org/10.1007/s13204-015-0454-2.
628 [48] Tributsch, H, Fiechter, S. The material strategy of fire-resistant tree barks. High

629 Performance Structures and Materials IV 2008;97:43-52.

630 [49] Tondi, G, Wieland, S, Wimmer, T, Thévenon, MF, Pizzi, A, Petutschnigg, A.
631 Tannin-boron preservatives for wood buildings: mechanical and fire properties.
632 European Journal of Wood and Wood Products 2012;70(5):689-696.
633 https://xs.scihub.ltd/https://doi.org/10.1007/s00107-012-0603-1.

634 [50] Pantoja-Castro MA, González-Rodríguez H. Study by infrared spectroscopy and
635 thermogravimetric analysis of tannins and tannic acid. Revista latinoamericana de
636 química 2011;39(3):107-112.

637 [51] Xia Z, Singh A, Kiratitanavit W, Mosurkal R, Kumar J, Nagarajan R. Unraveling
638 the mechanism of thermal and thermo-oxidative degradation of tannic acid
639 2015;605:77-85. https://doi.org/10.1016/j.tca.2015.02.016.

640 [52] Xi X, Pizzi A, Delmotte L. Isocyanate-Free Polyurethane Coatings and Adhesives
641 from Mono- and Di-Saccharides. Polymers 2018;10(4):402.
642 https://doi.org/10.3390/polym10040402.

643 [53] Zhou X, Li B, Xu Y, Essawy H, Wu Z, Du G. Tannin-furanic resin foam reinforced
644 with cellulose nanofibers (CNF). Industrial Crops and Products 2019;134:107-112.
645 https://doi.org/10.1016/j.indcrop.2019.03.052.

646 [54] Li J, Zhang A, Zhang S, Gao Q, Zhang W, Li J. Larch tannin-based rigid phenolic
647 foam with high compressive strength, low friability, and low thermal conductivity
648 reinforced by cork powder. Composites Part B: Engineering 2019;156:368-377.
649 https://doi.org/10.1016/j.compositesb.2018.09.005.

650 [55] Zhang A, Li J, Zhang S, Mu Y, Zhang W, Li J. Characterization and acid-catalysed
651 depolymerization of condensed tannins derived from larch bark. RSC Advances
652 2017;7(56):35135-35146. https://doi.org/10.1039/C7RA03410E.
653 [56] Santos OS, Coelho da Silva M, Silva VR, Mussel WN, Yoshida MI. Polyurethane
654 foam impregnated with lignin as a filler for the removal of crude oil from contaminated
655 water. Journal of hazardous materials 2017;324:406-413.
656 https://doi.org/10.1016/j.jhazmat.2016.11.004.
657 [57] Ranote S, Kumar D, Kumari S, Kumar R, Chauhan GS, Joshi V. Green synthesis
658 of Moringa oleifera gum-based bifunctional polyurethane foam braced with ash for
659 rapid and efficient dye removal. Chemical Engineering Journal 2019;361:1586-1596.
660 https://doi.org/10.1016/j.cej.2018.10.194.
661 [58] Cao Z-J, Liao W, Wang S-X, Zhao H-B, Wang Y-Z. Polyurethane foams with
662 functionalized graphene towards high fire-resistance, low smoke release, superior
663 thermal insulation. Chemical Engineering Journal 2019;361:1245-1254.
664 https://doi.org/10.1016/j.cej.2018.12.176.
665 [59] Merle J, Birot M, Deleuze H, Mitterer C, Carré H, Bouhtoury FC-E. New biobased
666 foams from wood byproducts. Materials & Design 2016;91:186-192.
667 https://doi.org/10.1016/j.matdes.2015.11.076.
668 [60] Tondi G, Pizzi A. Tannin-based rigid foams: Characterization and modification.
669 Industrial Crops and Products 2009;29(2-3):356-363.
670 https://doi.org/10.1016/j.indcrop.2008.07.003.

671 [61] Liu J, Chen R-Q, Xu Y-Z, Wang C-P, Chu F-X. Resorcinol in high solid phenol-
672 formaldehyde resins for foams production. Journal of Applied Polymer Science
673 2017;134(22):44881. https://doi.org/10.1002/app.44881.
674 [62] Li B, Feng S, Niasar H, Zhang Y, Yuan Z, Schmidt J, et al. Preparation and
675 characterization of bark-derived phenol formaldehyde foams. RSC Advances
676 2016;6(47):40975-40981. https://doi.org/10.1039/C6RA05392K.